Eco-Departure of Connected Vehicles With V2X Communication at Signalized Intersections

Shengbo Eben Li, *Member, IEEE*, Shaobing Xu, Xiaoyu Huang, Bo Cheng, and Huei Peng

***Abstract*—Eco-driving at signalized intersections has significant potential for energy saving. In this paper, we focus on eco-departure operations of connected vehicles equipped with an internal combustion engine and a step-gear automatic transmission. A Bolza-type optimal control problem (OCP) is formulated to minimize engine fuel consumption. Due to the discrete gear ratio, this OCP is a nonlinear mixed-integer problem, which is challenging to handle by most existing optimization methods. The Legendre pseudospectral method combining the knotting technique is employed to convert it into a multistage interconnected nonlinear programming problem, which then solves the optimal engine torque and transmission gear position. The fuel-saving benefit of the optimized eco-departing operation is validated by a passenger car with a five-speed transmission. For real-time implementation, a near-optimal departing strategy is proposed to quickly determine the behavior of the engine and transmission. When a string of vehicles are departing from an intersection, the acceleration of the leading vehicle(s) should be considered to control the following vehicles. This issue is also addressed in this paper.**

***Index Terms*—Connected vehicles, eco-departure, eco-driving, optimal control, pseudospectral method.**

I. Introduction

CONNECTED vehicle (CV) technologies are being developed to improve transportation system safety, mobility, and sustainability [1]. CVs equipped with wireless communication devices can exchange information with adjacent vehicles (V2V) and road infrastructures (V2I) [2], [3]. V2X (V2V, V2I, and beyond) enables new functions such as parking assist, remote diagnostics, infotainment, autonomous emergency braking, self-driving vehicles, and eco-driving [1].

Manuscript received April 20, 2015; revised July 10, 2015 and August 25, 2015; accepted September 19, 2015. Date of publication September 29, 2015; date of current version December 14, 2015. This work was supported in part by the National Natural Science Foundation of China under Grant 51205228 and Grant 51575293, and also in part by the Tsinghua University Initiative Scientific Research Program under Grant 2012THZ0. The review of this paper was coordinated by Guest Editors.

S. E. Li, S. Xu, and B. Cheng are with the State Key Laboratory of Automotive Safety and Energy, Department of Automotive Engineering, Tsinghua University, Beijing 100084, China (e-mail: lisb04@gmail.com; xsbing2008@foxmail.com; chengbo@tsinghua.edu.cn). S. E. Li and S. Xu are co-first authors. *(Corresponding author: Bo Cheng.)*

X. Huang was with the Department of Mechanical and Aerospace Engineering, The Ohio State University, Columbus, OH 43210 USA. He is now with General Motors Research and Development, Warren, MI 48093 USA (e-mail: huang.638@osu.edu).

H. Peng is with the Department of Mechanical Engineering, University of Michigan, Ann Arbor, MI 48109 USA, and also with the State Key Laboratory of Automotive Safety and Energy, Department of Automotive Engineering, Tsinghua University, Beijing 100084, China (e-mail: hpeng@umich.edu).

Color versions of one or more of the figures in this paper are available online at http://ieeexplore.ieee.org.

Digital Object Identifier 10.1109/TVT.2015.2483779

Eco-driving assistance/automation was estimated to have the potential of saving 10%–20% fuel consumption, which can translate to 750 million barrels of oil per year worldwide [4]–[6]. In an early attempt of eco-driving assistance, Boriboonsomsin *et al.* provided advices (e.g., shift gear timing and softer accelerate) to drivers and achieved a fuel benefit up to 24% [6]. Barth and Boriboonsomsin collected traffic flow data (e.g., speed and density) to generate a proper target cruising speed, which is recommended to drivers to reduce congestion and smooth traffic flow, resulting in a 10%–20% fuel reduction [7]. Eco-driving must take the traffic environment into account, such as road profile, surrounding vehicles, and traffic signals [8]. Connected vehicles make it possible to collect and share the environmental information and are the promising platform to realize eco-driving.

Eco-driving can be implemented in different driving situations, such as (a) free cruising on up/downhill, (b) car following, and (c) stop&go at signalized intersections [7]–[9]. In the first two scenarios, using the information of road profile and lead vehicles provided by V2X, more efficient driving strategies can be designed to avoid inefficient engine operations and unnecessary idling/brake, thus saving fuel [9]. Some related work can be founded in [10]–[12]. In this paper, we focus on the scenario (c).

Eco-driving at signalized intersections has considerable fuel-saving potential [13]. Asadi and Vahidi observed up to 47% fuel reduction in a simulation case [15]. The "Applications for the Environment: Real-Time Information Synthesis (AERIS)," which is a project supported by the U.S. Department of Transportation, regards the eco-operation at intersections as one of the most common and high potential applications. The key focus was to avoid improper acceleration and prolonged idling [14], [15]. This can be achieved through well-planned vehicle speed trajectories with the following two methods: (a) global optimization for a multi-intersection corridor; or (b) receding finite-horizon optimization for each upcoming single signal. In the first method, the information of traffic lights at all involved intersections is assumed to be known, and global search methods, such as dynamic programming or shortest path algorithm, are applied to compute the vehicle speed profile. Examples can be found in [8] and [14]. For the second approach, with adopting the state of the traffic light at a single intersection, receding horizon predictive controllers are designed to schedule the optimal velocity profile for minimizing fuel consumption or traveling time. Related works can be found in [15] and [16].

Instead of the aforementioned two approaches, we focus on a computationally inexpensive and easy-to-implement strategy that has clear operating rules. The strategy is divided

into two stages: eco-approach and eco-departure. In the eco-approach stage, parameters such as vehicle speed, distance to the intersection, and traffic signal phase are considered to decide to accelerate, coast, or decelerate [12], [17], [18]. Most existing works studied eco-approach, and eco-departure needs to be strengthened. This paper concentrates on the fuel-optimal departing operation for connected vehicles with step-gear transmission. The results can be used to guide drivers and automatic control systems to select proper acceleration profiles and transmission gear shifting points to restore vehicle speed after the stop or coasting down in the approaching stage while achieving minimum fuel consumption.

The contributions of this paper include the following:

a) We studied the fuel-optimal departing operation of connected vehicles, including the behaviors of the engine and transmission. The studied vehicle comes equipped with an internal combustion engine (ICE) and an automatic mechanical transmission (AMT). To quantitatively obtain the optimal operation of the engine and transmission, we formulate a Bolza-type optimal control problem (OCP) to minimize the engine fuel consumption. Due to the discrete nature of the transmission gear ratio, the OCP is a nonlinear mixed-integer control problem [19]. We employ the Legendre pseudospectral method combined with the knotting technique to solve this problem.

b) We proposed a near-optimal speed-based strategy that is suitable for real-time implementation. This strategy can determine the acceleration (or engine torque) profile, gear positions, and gear shifting points very quickly, with only slightly deteriorated fuel saving as compared with the original nonlinear numerical optimization.

c) Considering the constraints arising from the front vehicles, a control rule combining the safety-guaranteed car-following model and the fuel-prioritized departing operation is also proposed for multivehicle scenarios.

The remainder of this paper is organized as follows: Section II describes the fuel-optimal eco-departure problem, Section III presents the method for solving the problem; Section IV analyzes the optimization results, Section V designs the near-optimal eco-departure strategy for the first vehicle departing from an intersection, Section VI presents the eco-departure strategy for the impeded following vehicles, and Section VII concludes this paper.

II. Eco-Departing Problem Statement

By using the V2X technologies, information such as traffic signal phasing can be collected and shared to achieve better fuel economy, as shown in Fig. 1. Eco-approaching strategies can minimize stopping or idling time, and avoid unnecessary acceleration, by manipulating vehicle speed trajectory. However, stopping at a signal may be unavoidable in some cases. After a stop, eco-departure maneuvers can be executed. The first vehicle can freely depart without a lead vehicle impeding its motion, while all the following vehicles must consider their lead vehicles, which might end up impeding their motions. In solving all these optimal departing problems, we assume that vehicle motion data are collected and shared through V2V.

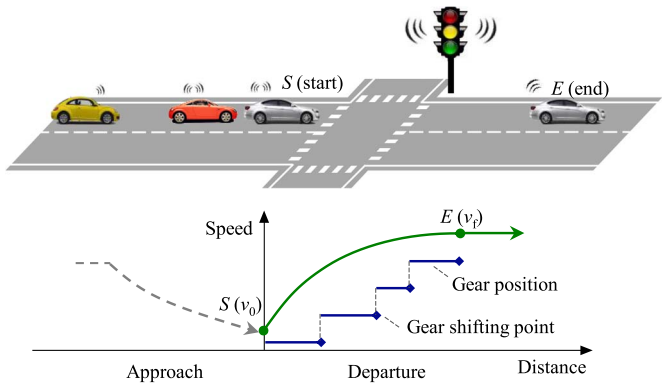

Fig. 1. Eco-departure problem at a signalized intersection.

The goal of this paper is to obtain the fuel-optimal eco-departure strategies for both the free (first vehicle) and constrained (all subsequent) vehicles. The optimal operation of the free vehicle is solved first, which also becomes the foundation for the constrained vehicles. Therefore, in Sections II–V, we focus on studying the problem for the free vehicle. The control rule for the constrained vehicles is then presented in Section VI.

The studied vehicle uses a 2.0-L engine, a 5-speed AMT, and a wet clutch. Since the objective is to maximize fuel economy, we formulate an OCP, with engine torque and transmission gear as the control inputs, as shown in Fig. 1. The initial speed v_0 is known (zero or higher). The terminal speed $v_\mathrm{f} > v_0$ is suggested by road infrastructures, which can collect traffic flow data to estimate a proper v_f and then transfer it to the connected vehicle by V2R communication. For multiple vehicles, these necessary data, such as vehicle speed, acceleration, and location, are exchanged by V2V communication. In the following, the performance index and vehicle dynamics of the eco-departing OCP are presented.

A. Equivalent Fuel Consumption Index

In the departing scenario, total fuel consumption from point S to E in Fig. 1 is defined as

$$J_\mathrm{SE} = \int_0^{t_\mathrm{f}} \mathcal{F}_\mathrm{e}(T_\mathrm{e}, w_\mathrm{e})\mathrm{d}t \tag{1}$$

where t_f is the final time; and T_e, w_e, and $\mathcal{F}_\mathrm{e}(\cdot)$ are the engine torque, speed, and fuel injection rate, respectively.

J_SE cannot be used alone to measure the fuel economy of different departing strategies, owing to the fact that the travel distance may vary substantially among different strategies. To have a fair comparison, the vehicle is made to run to a same virtual destination, as shown in Fig. 2(a). The vehicle is assumed to accelerate from point S to E first and then cruise to the virtual destination (i.e., point D) at speed v_f.

The fuel consumption of cruising from point E to D is called virtual fuel consumption J_ED, which is defined as

$$J_\mathrm{ED} = \frac{s_\mathrm{SD} - s_\mathrm{SE}}{v_\mathrm{f}} \mathcal{F}_\mathrm{C}(v_\mathrm{f}) \tag{2a}$$

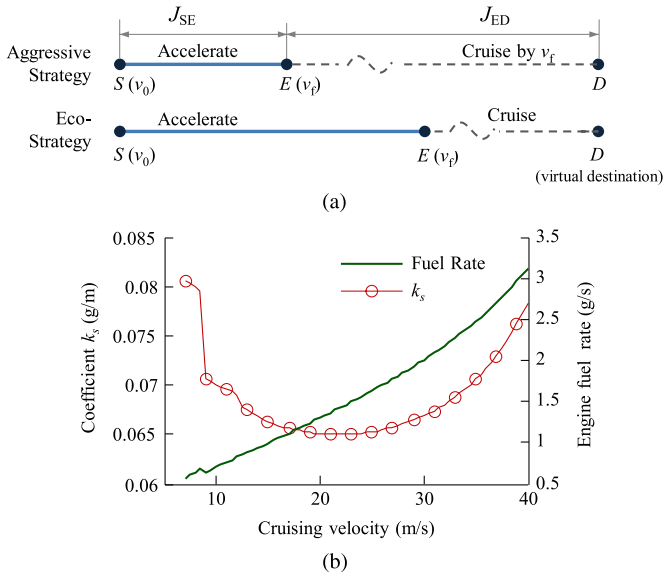

Fig. 2. Explanation of the performance index. (a) Concept of equivalent fuel consumption index. (b) Coefficient k_s and fuel rate at various velocities.

where $s_{\mathrm{SD}}/s_{\mathrm{SE}}$ is the distance of section SD/SE, $\mathcal{F}_{\mathrm{C}}(v_{\mathrm{f}})$ is the engine fuel rate cruising at speed v_{f}. In a particular departing task, s_{SD}, v_{f}, and $\mathcal{F}_{\mathrm{C}}(v_{\mathrm{f}})$ are constant; thus, the term $s_{\mathrm{SD}}\mathcal{F}_{\mathrm{C}}(v_{\mathrm{f}})/v_{\mathrm{f}}$ is constant for different strategies and can be omitted in the optimization. Therefore, (2a) is simplified as

$$J_{\mathrm{ED}} = -k_s s_{\mathrm{SE}}, \quad k_s = \frac{\mathcal{F}_{\mathrm{C}}(v_{\mathrm{f}})}{v_{\mathrm{f}}} \tag{2b}$$

where k_s is called the correction coefficient of distance, as shown in Fig. 2(b).

A performance index called equivalent fuel consumption J is then proposed, i.e.,

$$J = J_{\mathrm{ED}} + J_{\mathrm{SE}} = -k_s s_{\mathrm{SE}} + \int_0^{t_{\mathrm{f}}} \mathcal{F}_{\mathrm{e}}(T_{\mathrm{e}}, w_{\mathrm{e}})\mathrm{d}t. \tag{3}$$

The engine tested fuel map proved by a motor company is adopted and fitted by a 2-D fourth-order polynomial to obtain engine fuel rate $\mathcal{F}_{\mathrm{e}}$, i.e.,

$$\mathcal{F}_{\mathrm{e}}(T_{\mathrm{e}}, w_{\mathrm{e}}) = \sum_{i=0}^{4}\sum_{j=0}^{i} k_{\mathcal{F},1+j+\Sigma_0^i n} T_{\mathrm{e}}^{i-j} w_{\mathrm{e}}^{j} \tag{4}$$

where $k_{\mathcal{F},\#}$ are the fitting coefficients. The engine brake-specific fuel consumption (BSFC) is shown in Fig. 3, along with the sweet spot and maximum torque $T_{\max}$. The Efficient Line, i.e., collection of the most efficient points for varying engine speeds, is also highlighted in Fig. 3.

The steady-state engine map does not accurately predict the fuel consumption in dynamic driving. The transient dynamics can cause wall wetting and reduction in volumetric efficiency, thus reducing actual output torque compared to the statically

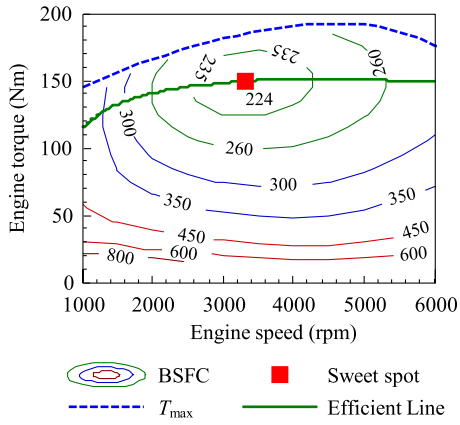

Fig. 3. Engine BSFC.

calibrated engine test data. A correction term related to the derivative of engine speed is adopted here [21] as follows:

$$T_{\mathrm{ed}} = T_{\mathrm{e}}\left(1 - \gamma_{\mathrm{d}}\frac{\mathrm{d}w_{\mathrm{e}}}{\mathrm{d}t}\right) \tag{5}$$

where γ_{d} is the correction coefficient, and T_{ed} is the dynamic effective engine torque.

B. Vehicle Longitudinal Dynamics

The following assumptions are made.

1) The high-order dynamics of small rotating parts such as the flywheel and clutch are ignored.
2) The gear shifting is executed instantaneously, and the clutch slip is neglected.

In an eco-departure process, the vehicle distance s, velocity v, and acceleration a satisfy

$$\begin{aligned} \dot{s} &= v \\ \dot{v} &= a. \end{aligned} \tag{6}$$

Based on the force balance equation [20], one obtains

$$\frac{i_0\eta_{\mathrm{T}}}{r_w} i_{\mathrm{g}} T_{\mathrm{ed}} = \delta_{i_{\mathrm{g}}} M\dot{v} + k_a v^2 + k_f \tag{7}$$

where i_{g} and i_0 are the gear ratio of the transmission and final gears, respectively; r_w is the tire effective radius; η_{T} is the total efficiency of the driveline; $\delta_{i_{\mathrm{g}}}$ is the lumped rotational inertial coefficient; $k_a = 0.5C_{\mathrm{D}}\rho_{\mathrm{a}}A_v$, and $k_f = Mgf$ are related to the aerodynamic drag force and rolling resistance; C_{D} is the aerodynamic drag coefficient; ρ_{a} is the air density, A_v is the frontal area of the vehicle; f is the rolling resistance coefficient; M and g represent the vehicle mass and gravity constant.

The engine speed w_{e} (in revolutions per minute) and vehicle speed v(m/s) are governed by the following relationship:

$$w_{\mathrm{e}} = k_w v i_{\mathrm{g}}, \quad k_w = \frac{30}{\pi r_w} \tag{8}$$

where k_w is the lumped coefficient.

TABLE I
KEY PARAMETERS OF VEHICLE DYNAMICS

Parameters	Value	Parameters	Value
C_{D}	0.316	η_{T}	0.9
A_v	2.22 m^2	γ_{d}	0.003 $\mathrm{s}^2/\mathrm{rad}$
ρ_{a}	1.226 kg/m^3	r_w	0.307 m
M	1600 kg	F_{z}	3920 N
f	0.028	$w_{\min}$	1000 rpm
i_0	3.863	$w_{\max}$	6000 rpm
i_{g}	3.620, 1.925, 1.285, 0.933, 0.692		
$\delta_{i_{\mathrm{g}}}$	1.322, 1.112, 1.067, 1.049, 1.041		

At a particular gear position, the gear ratio is fixed; thus, (5) is simplified to

$$T_{\mathrm{ed}} = T_{\mathrm{e}}(1 - \gamma_{\mathrm{d}} k_w i_{\mathrm{g}} \dot{v}). \tag{9}$$

Combining (6), (7), and (9), the vehicle longitudinal motion equations are expressed as follows:

$$\begin{aligned} \dot{s} &= v \\ \dot{v} &= \frac{i_{\mathrm{g}} i_0 \eta_{\mathrm{T}} T_{\mathrm{e}}/r_w - k_a v^2 - k_f}{\delta_{i_{\mathrm{g}}} M + i_0 \eta_{\mathrm{T}} \gamma_{\mathrm{d}} k_w i_{\mathrm{g}}^2 T_{\mathrm{e}}/r_w}. \end{aligned} \tag{10}$$

Inequality constraints of the system include the following: (a) physical limits of the powertrain, (b) ride comfort, and (c) road friction limit. The first one includes the engine speed, engine torque, and transmission gear ratio, i.e.,

$$\begin{aligned} & w_{\min} \le w_{\mathrm{e}} \le w_{\max} \\ & 0 < T_{\mathrm{e}} \le T_{\max}(w_{\mathrm{e}}) \\ & i_{\mathrm{g}} \in \{i_{\mathrm{g}1}, i_{\mathrm{g}2}, i_{\mathrm{g}3}, i_{\mathrm{g}4}, i_{\mathrm{g}5}\}. \end{aligned} \tag{11}$$

The second one limits the vehicle acceleration in departing as follows:

$$a_{\min} \le a \le a_{\max}. \tag{12}$$

Finally, the road friction limit

$$\frac{i_0 \eta_{\mathrm{T}}}{2 F_z r_w} i_{\mathrm{g}} T_{\mathrm{e}} \le \lambda_{\max} \tag{13}$$

where F_z is the load of a single driving wheel ignoring the mass transfer during accelerating, and $\lambda_{\max}$ is the maximum road friction coefficient.

Except for the engine model introduced in Section II-A, the other parameters are listed in Table I.

C. Eco-Departing Control Problem

The resulting fuel-optimal departing problem is stated as follows:

$$\min J = -k_s(v_{\mathrm{f}}) s_{\mathrm{f}} + \int_0^{t_{\mathrm{f}}} \mathcal{F}_{\mathrm{e}}(T_{\mathrm{e}},\ w_{\mathrm{e}}) \mathrm{d}t$$

subject to

$$\begin{aligned} \dot{s} &= v \\ \dot{v} &= \frac{i_{\mathrm{g}} i_0 \eta_{\mathrm{T}} T_{\mathrm{e}}/r_w - k_a v^2 - k_f}{\delta_{i_{\mathrm{g}}} M + i_0 \eta_{\mathrm{T}} \gamma_{\mathrm{d}} k_w i_{\mathrm{g}}^2 T_{\mathrm{e}}/r_w} \\ a_{\min} &\le \dot{v} \le a_{\max} \\ i_{\mathrm{g}} T_{\mathrm{e}} &\le 2\lambda_{\max} F_z r_w/(i_0 \eta_{\mathrm{T}}) \\ w_{\min} &\le w_{\mathrm{e}} \le w_{\max} \\ 0 &< T_{\mathrm{e}} \le T_{\max}(w_{\mathrm{e}}) \\ i_{\mathrm{g}} &\in \{i_{\mathrm{g}1}, i_{\mathrm{g}2}, i_{\mathrm{g}3}, i_{\mathrm{g}4}, i_{\mathrm{g}5}\}. \end{aligned} \tag{14}$$

The states are the distance s and velocity v, denoted by $\boldsymbol{x} = (s, v)^{\mathrm{T}}$. The control inputs include the engine torque T_{e} and gear ratio i_{g}, denoted by $\boldsymbol{u} = (T_{\mathrm{e}}, i_{\mathrm{g}})^{\mathrm{T}}$. Due to the discontinuity of the control input i_{g} and strong nonlinearity in the dynamics, the resulting nonlinear mixed-integer problem is challenging to solve. To address this problem, we employ the Legendre pseudospectral method and knotting technique to convert it into a nonlinear programming (NLP) problem for more accurate numerical calculation.

III. LEGENDRE PSEUDOSPECTRAL METHOD AND KNOTTING TECHNIQUE

The Legendre pseudospectral method (LPM) is a global collocation method for solving smooth OCPs [22]–[24]. Its fundamental is to discretize the OCP at orthogonal collocation points, then use global rather than local interpolating polynomials to approximate the states and control inputs, and convert the OCP into an associated NLP. Compared to the conventional methods (e.g., shooting method), LPM has better accuracy and convergence speed [22]. It should be noted that LPM is highly accurate only for smooth problems [23]; thus, it cannot handle the nonsmooth eco-departing problem shown in (14). To conquer the discontinuity, we apply the knotting technique with the prior knowledge of gear shifting to convert this problem.

In the departing process, i.e., accelerating to a higher given speed, the operation of the AMT follows these principles.

1) The AMT sequentially upshifts from a lower gear position to a higher one.
2) At the beginning of departing, "kick-down" is allowed, i.e., the AMT can instantaneously shift down to a lower gear position.

With the aforementioned rules, the nonsmooth problem is converted into several smooth subproblems; each of them corresponds to a gear position [23]. To ensure continuity of states (e.g., vehicle speed and distance), constraints are added between the consecutive stages to link the local trajectories [23]. The optimal results, such as engine torque, transmission gears, and shifting points, are obtained by the simultaneous optimization of the local NLPs. This technique can avoid accuracy loss compared with using one finite-order polynomial to approximate a nonsmooth trajectory.

To implement the knotting technique, we first determine the initial gear i_{gs} and final gear i_{gf}. The admissible minimum and maximum gear ratios for a given speed v are denoted by $i_{\mathrm{g,min}}(v)$ and $i_{\mathrm{g,max}}(v)$, respectively. Since the optimal i_{gs} and i_{gf} are unknown, we set the initial (final) gear to be the admissible minimum (maximum) gear, i.e.,

$$\begin{aligned} i_{\mathrm{gs}} &= i_{\mathrm{g,min}}(v_0) \\ i_{\mathrm{gf}} &= i_{\mathrm{g,max}}(v_{\mathrm{f}}). \end{aligned} \tag{15}$$

The OCP is then divided into Q phases, where Q equals to the number of involved gears. The initial time, $(Q-1)$ break points, and final time are denoted by $T_0, T_1, T_2, \ldots, T_{Q-1}, T_Q$, respectively. The time gaps between two sequential break points are forced to satisfy

$$T_q - T_{q-1} \geq \delta_t \tag{16}$$

where $q = 1, 2, \ldots, Q$, δ_t is a scalar and set to 0.25 s, here. If the duration at a specific gear equals to δ_t, the gear is actually skipped, which indicates that this optimization framework allows "skip-shift." The process of converting the eco-departure problem (14) by the LPM and knotting technique is stated as follows.

a) Conversion of time intervals: The time interval $[T_{q-1}, T_q]$ is transformed into a canonical interval $[-1,1]$ by

$$\tau = \frac{2t - (T_q + T_{q-1})}{T_q - T_{q-1}}, \quad \tau \in [-1, 1]. \tag{17}$$

b) Collocation points and approximation: The LPM uses Legendre–Gauss–Lobatto collocation points. They are the roots of the derivative of the Nth-order Legendre polynomial and two end points -1 and 1. The collocation points at the qth phase are denoted by $\tau_{q,i}$, where $i = 0, 1, \ldots, N_q$. Thus, the states s and v are discretized as

$$\boldsymbol{X}_q = \begin{bmatrix} S_{q,0} & S_{q,1} & \cdots & S_{q,N_q} \\ V_{q,0} & V_{q,1} & \cdots & V_{q,N_q} \end{bmatrix}. \tag{18}$$

The engine torque T_{e} is discretized to $\mathbb{T}_{q,i}$ in the same way. Note that only the discretized states and control inputs are optimized; the dynamic $\boldsymbol{x}_q(\tau)$ and $T_{\mathrm{e}}(\tau)$ are obtained by Lagrange interpolation at collocations points, i.e.,

$$\begin{aligned} \boldsymbol{x}_q(\tau) &\approx \sum_{i=0}^{N_q} L_{q,i}(\tau) \boldsymbol{X}_{q,i} \\ T_{\mathrm{e}}(\tau) &\approx \sum_{i=0}^{N_q} L_{q,i}(\tau) \mathbb{T}_{q,i} \end{aligned} \tag{19}$$

where $L_{q,i}(\tau)$ are the Lagrange basis polynomials.

c) Conversion of vehicle dynamics: The state derivatives can be calculated from

$$\dot{x}_q(\tau_{q,k}) = \sum_{i=0}^{N_q} \dot{L}_{q,i}(\tau_{q,k}) \boldsymbol{X}_{q,i} = \sum_{i=0}^{N_q} D_{ki}^q \boldsymbol{X}_{q,i} \tag{20}$$

where $k = 0, 1, 2, \ldots, N_q$, and $\boldsymbol{D}^q$ is the differentiation matrix with explicit expression [24].

Then, the vehicle dynamics (10) are converted to a series of equality constraints at the collocation points as follows:

$$\begin{aligned} \sum_{i=0}^{N_q} D_{ki}^q S_{q,i} &= \Delta T_q V_{q,k} \\ \sum_{i=0}^{N_q} D_{ki}^q V_{q,i} &= \Delta T_q \frac{i_{\mathrm{g}q} i_0 \eta_{\mathrm{T}} \mathbb{T}_{q,k}/r_w - k_a V_{q,k}^2 - k_f}{\delta_{i_{\mathrm{g}q}} M + i_0 \eta_{\mathrm{T}} \gamma_{\mathrm{d}} k_w i_{\mathrm{g}q}^2 \mathbb{T}_{q,k}/r_w} \end{aligned} \tag{21}$$

where $\Delta T_q = (T_q - T_{q-1})/2$, and $i_{\mathrm{g}q}$ denotes the gear ratio in the qth phase.

d) Conversion of performance index: The integration part of the cost function is numerically calculated by the Gaussian–Lobatto quadrature. Then, the Bolza-type cost function is converted as follows:

$$J = -k_s S_{Q,N_Q} + \sum_{q=1}^{Q} \Delta T_q \sum_{i=0}^{N_q} w_{q,i} \mathcal{F}_{\mathrm{e}}(\mathbb{T}_{q,i}, \mathbb{W}_{q,i}) \tag{22}$$

where $\mathbb{W}_{q,i}$ is the discretized engine speed, and $w_{q,i}$ is the weighting coefficient of the Gaussian–Lobatto quadrature [24].

e) Connection constraints: To ensure the continuity of s and v, the following connection constraints are added:

$$\begin{aligned} S_{q',N_{q'}} - S_{q'+1,0} &= 0 \\ V_{q',N_{q'}} - V_{q'+1,0} &= 0 \end{aligned} \tag{23}$$

where $q' = 1, 2, \ldots, Q-1$.

After the aforementioned steps, the fuel-optimal eco-departure problem (14) is converted into the following NLP problem:

$$J = -k_s S_{Q,N_Q} + \sum_{q=1}^{Q} \Delta T_q \sum_{i=0}^{N_q} w_{q,i} \mathcal{F}_{\mathrm{e}}(\mathbb{T}_{q,i}, \mathbb{W}_{q,i})$$

subject to

$$\begin{aligned} \sum_{i=0}^{N_q} D_{ki}^q S_{q,i} &= \Delta T_q V_{q,k} \\ \sum_{i=0}^{N_q} D_{ki}^q V_{q,i} &= \Delta T_q \frac{i_{\mathrm{g}q} i_0 \eta_{\mathrm{T}} \mathbb{T}_{q,k}/r_w - k_a V_{q,k}^2 - k_f}{\delta_{i_{\mathrm{g}q}} M + i_0 \eta_{\mathrm{T}} \gamma_{\mathrm{d}} k_w i_{\mathrm{g}q}^2 \mathbb{T}_{q,k}/r_w} \\ 0 &= S_{q',N_{q'}} - S_{q'+1,0} \\ 0 &= V_{q',N_{q'}} - V_{q'+1,0} \\ a_{\min} \leq \frac{1}{\Delta_q} \sum_{i=0}^{N_q} D_{ki}^q V_{q,i} &\leq a_{\max} \\ i_{\mathrm{g}q} \mathbb{T}_{q,k} &\leq \frac{2\lambda_{\max} F_z r_w}{(i_0 \eta_{\mathrm{T}})} \\ w_{\min} \leq \mathbb{W}_{q,k} &\leq w_{\max} \\ 0 < \mathbb{T}_{q,k} &\leq T_{\max}(\mathbb{W}_{q,i}) \\ \delta_t &\leq T_q - T_{q-1} \\ i_{\mathrm{g}} &\in \{i_{\mathrm{g}1}, i_{\mathrm{g}2}, i_{\mathrm{g}3}, i_{\mathrm{g}4}, i_{\mathrm{g}5}\} \end{aligned} \tag{24}$$

where $k, i = 0, 1, 2, \ldots, N_q$; $q = 1, 2, \ldots, Q$; and $q' = 1, 2, \ldots, Q-1$. The variables to be optimized include travel distance $S_{q,k}$, vehicle speed $V_{q,k}$, engine torque $\mathbb{T}_{q,k}$, gear shifting

TABLE II
DEPARTING TASKS WITH CONSTRAINTS

Task	Parameter			
	v_0 (m/s)	v_f (m/s)	a_{max} (m/s^2)	λ_{max}
Nominal	2.5	25	--	0.8
Comfort	2.5	25	0.5	0.8
Low friction	2.5	25	--	0.3

points $T_1, T_2, \ldots, T_{Q-1}$, and final time T_Q. This resulting NLP is essentially a high-dimensional sparse optimization problem and can be solved by the sequential quadratic programming algorithm [25].

IV. OPTIMIZATION RESULTS AND ANALYSES

A. Optimization of the Eco-Departure Operation

To understand the eco-departure operation, a typical scenario, i.e., departing from standstill to the economy cruising speed, is studied. Three tasks with different constraints, which are called "Nominal," "Comfort," and "Low friction," are set in Table II. The task "Nominal" is a baseline; "Comfort" limits the maximum acceleration to 0.5 m/s^2 to ensure ride comfort; and the "Low friction" case assumes that the road is icy. The initial and final gears are set to I and V based on (15). To avoid the complex start-up phase of a vehicle with ICE, the initial speed is set to 2.5 m/s rather than zero.

The number of collocation points in each phase is set to 10. The optimal vehicle speed, acceleration, utilized friction, engine operating points, and cumulative fuel consumption of the three tasks are shown in Fig. 4; the gear shifting points are marked by diamond-dots.

In the "Nominal" case, the five transmission gears are sequentially used, and skip-shift does not happen; the higher the gear position, the smaller the acceleration, as shown in Fig. 4(b). This varying optimal acceleration allows the engine to operate efficiently, as shown in Fig. 4(e). The engine torque is around 70%–85% of the maximum torque, and the engine speed is in the range of 1200–3000 r/min.

In the "Comfort" case, due to the constraint on maximum acceleration, the accelerations used in gears I to III deviate from the optimum and are limited to 0.5 m/s^2 in Fig. 4(b). This forced the engine to operate inefficiently, as shown in Fig. 4(e), thus leading to 8.4% higher fuel consumption compared to the "Nominal" case.

In the "Low friction" case, to avoid slippage on the icy road, the accelerations at gears I and II also deviate from the optimum, with the utilized friction approaching the road limit, as shown in Fig. 4(c). However, this constraint on λ_{max} has a weaker effect on fuel economy; the velocity trajectory and engine operating points are much closer to the optimum than that of the "Comfort" case, resulting in only 1.6% more fuel consumption.

The aforementioned optimization results indicate the effectiveness of the proposed method for eco-departure. However, this method is applicable for offline calculation only. The computing time is on the order of seconds to tens of seconds, depending on the number of collocation points, initial values, and complexity (e.g., constraints) of the problem. For real-time implementation, a practical near-optimal departing strategy is proposed in Section V.

B. Effect of the Final Speed

Depending on the traffic status, the final departing velocity can vary in a large range. To understand its effect on the departing operation, three cases with different final speeds, which are denoted as "Low," "Medium," and "High" in Table III, are studied.

Due to the different final speeds, the values of the correction coefficient k_s are 0.0701, 0.0648, and 0.0706 g/m, respectively. The optimization results of these three cases are shown in Fig. 5. We can see that the optimal gears, shifting points, and accelerations are distinct; in the "Medium" case, a higher acceleration and delayed shift compared to the "High" case are used. The optimal acceleration and gear shifting points depend on both the current speed and the final speed, making it challenging to determine proper acceleration profiles and gear positions promptly. This issue is addressed by the near-optimal strategy to be presented in the following.

C. Kick-Down Strategy

Kick-down strategy means that the transmission can instantaneously downshift to a lower gear, which enables better acceleration. Imagine that a vehicle coasted down to the intersection and is departing when the traffic light turns green; to decrease the engine drag torque in the coasting stage, the transmission was in a high gear position. In the departing stage, the vehicle can accelerate using the high gear directly or kick down to a lower gear first. The studied cases are set in Table IV; the initial gears are III and I, respectively, where gear I is used by the kick-down operation. The optimal gear-shifting operation, acceleration trajectories, and engine operating points of the two cases are shown in Fig. 6.

In the case of "w/ kick-down," gear I lasts only 0.25 s, indicating that skip-shift happens, as shown in Fig. 6(a). The equivalent fuel consumption of "w/ kick-down" and "w/o kick-down" is 10.56 and 11.34 g, respectively; thus, the former achieves a better fuel economy with 6.88% fuel savings. This result can be explained by Fig. 6(b). When $v \in [7, 12.2]$ m/s, gear III is used in the "w/o kick-down" case, and the engine operates at an inefficient area, marked by the triangles. If "kick-down" is taken, gears I and II are used; lower gears I and II can move these inefficient engine operating points to a more efficient area, marked by the circles. In fact, we argue that the kick-down strategy always leads to large search space and, thus, better fuel economy than the strategy of "without kick-down."

In reality, some drivers who drive a vehicle with traditional manual transmission, or tiptronic transmission, may be reluctant to downshift before departing, which even makes the engine operate at its physical limits and thus leads to severe vibrations. The aforementioned results can inspire them to select a proper operation on transmission if the initial gear is in the wrong position.

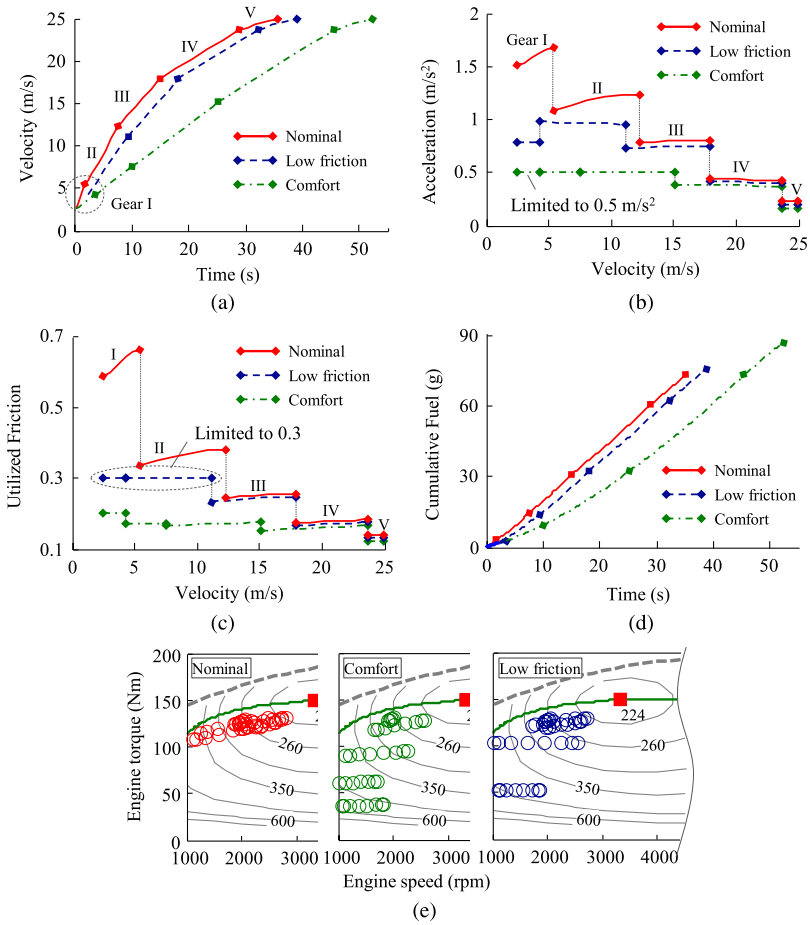

Fig. 4. Optimization results of "Nominal," "Comfort," and "Low friction." (a) Vehicle velocity. (b) Vehicle acceleration. (c) Utilized road friction. (d) Engine operating points. (e) Cumulative fuel consumption.

TABLE III
DEPARTING TASKS WITH DIFFERENT FINAL SPEEDS

Task	Parameter			
	v_0 (m/s)	v_f (m/s)	$a_{\min}$ (m/s^2)	$\lambda_{\max}$
Low	5	10	0.2	0.8
Medium	5	25	0.2	0.8
High	5	35	0.2	0.8

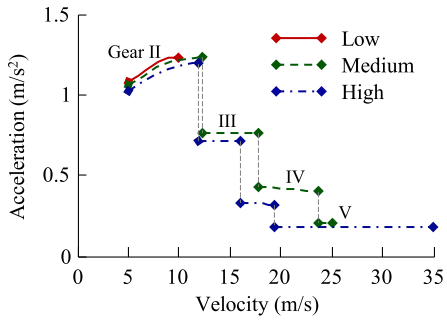

Fig. 5. Vehicle acceleration profiles of "Low," "Medium," and "High" cases.

D. Fuel-Saving Potential of the Optimized Strategy

To illustrate the fuel-saving potential of the optimization-based strategies, we compare the optimized eco-departing operation of the case "Nominal" in Section IV-A with the following departing strategies:

TABLE IV
DEPARTING TASKS WITH KICK-DOWN STRATEGY

Task	Parameter				
	v_0 (m/s)	v_f (m/s)	i_{gs}	i_{gf}	λ_{max}
w/o kick-down	7	15	III	III	0.8
w/ kick-down	7	15	I	III	0.8

1) departing with the engine always operating on the efficient line (see Fig. 3), denoted by S_{EL};
2) departing with maximum acceleration, denoted by $S_{\max}$. The optimal control is also solved by the proposed method using the following performance index in problem (14):

$$\min J = t_f; \tag{25}$$

3) departing with fixed acceleration 0.2, 0.8, and 1.5 m/s^2, denoted by $S_{0.2}$, $S_{0.8}$, and $S_{1.5}$, respectively. They stand for mild, medium, and aggressive departing.

The acceleration trajectories of the six strategies are shown in Fig. 7, and their key performance indexes, including the duration, distance, and fuel consumption, are listed in Table V.

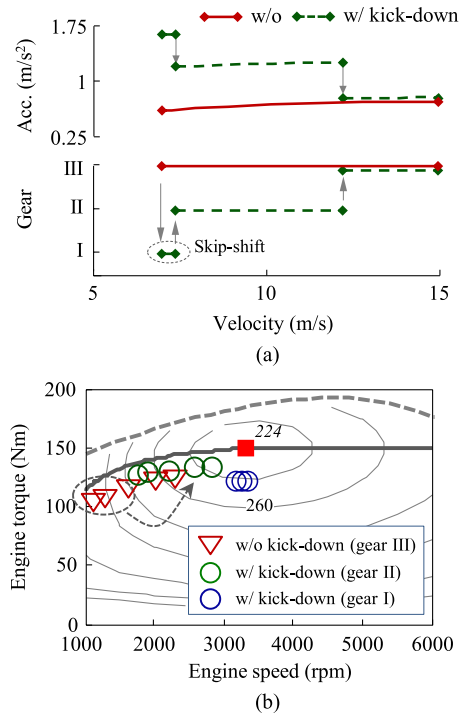

Fig. 6. Comparison of departing operation with and without kick-down strategies. (a) Vehicle acceleration and the operation of transmission. (b) Engine operating points when $\nu \in [7, 12.2]$ m/s.

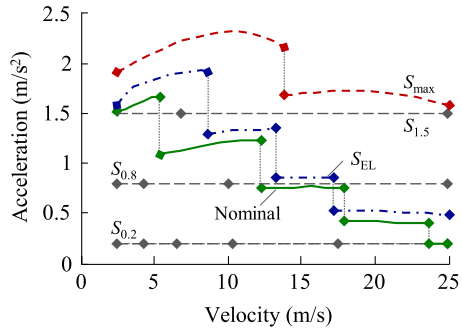

Fig. 7. Acceleration profiles of the six departing strategies.

TABLE V
KEY PERFORMANCE INDEXES OF THE SIX STRATEGIES

	Nomi.	S_{EL}	S_{max}	$S_{0.2}$	$S_{0.8}$	$S_{1.5}$
Total time (s)	35.65	26.60	11.77	112.50	28.12	15.00
Distance (m)	622.4	447.4	170.1	1546.9	386.7	206.2
Total J_{SE} (g)	73.93	64.08	70.51	144.20	61.33	59.66
Virtual J_{ED} (g)	-40.62	-29.20	-11.10	-100.97	-25.24	-13.46
Equ. J (g)	33.31	34.88	59.41	43.24	36.09	46.20
Fuel Increment	-	4.7%	78.4%	29.8%	8.4%	38.7%

In Table V, it is clear that the departing distance varies significantly. The strategy S_{max} consumes almost the same amount of fuel as the "Nominal" case but travels a much shorter distance. The distance gap (452 m) actually needs 29.5 g more fuel to cruise. This result indicates that using total fuel J_{SE} only is not appropriate to evaluate the fuel economy of various operations, and the virtual fuel J_{ED} should be adopted to decrease the effects of traveling distance.

In terms of fuel economy, the two aggressive departing strategies S_{max} and $S_{1.5}$ perform worst, consuming 78.4% and 38.7% more fuel compared to the "Nominal" case; the mild departing operation $S_{0.2}$ also consumes 29.8% more fuel; while the medium operation $S_{0.8}$ only consumes 8.4% more. Comparing the strategy S_{EL} with "Nominal," the former is close to the optimum but still consumes 4.7% more fuel, which confirms that, while the engine efficiency is important, an engine-centric algorithm such as BSFC alone does not achieve best fuel economy; other factors such as engine dynamics and aerodynamic drag also play a role.

V. NEAR-OPTIMAL STRATEGY FOR REAL-TIME IMPLEMENTATION

As previously mentioned, the optimization method is effective to find the optimal eco-departure operation, but its heavy computation load makes it undesirable for real-time implementation. In this section, a near-optimal strategy that is easier for real-time implementation is proposed.

To be concise, we first assume that only one gear will be used for eco-departure. The problem (14) has fixed initial states $(s_0,\ v_0)$, free final distance s_f, free final time t_f, and fixed final speed v_f. We first convert this time-based problem into a speed-based problem (26), i.e.,

$$\min J = -k_s(v_f)s_f + \int_{v_0}^{v_f} \frac{\mathcal{F}_e(T_e, w_e)}{g(T_e, v)} dv$$

subject to

$$\begin{aligned} \frac{ds}{dv} &= \frac{v}{g(T_e, v)} \\ g(T_e, v) &= \dot{v} \\ &= \frac{i_g i_0 \eta_T T_e / r_w - k_a v^2 - k_f}{\delta_{i_g} M + i_0 \eta_T \gamma_d k_w i_g^2 T_e / r_w}. \end{aligned} \tag{26}$$

Its Hamiltonian is given by

$$H = \frac{\mathcal{F}_e(T_e, w_e)}{g(T_e, v)} + \lambda \frac{v}{g(T_e, v)} \tag{27}$$

where λ is the costate. Thus, we can obtain the necessary conditions of optimality, i.e.,

$$\frac{\partial H}{\partial T_e} = \frac{\partial}{\partial T_e}\left(\frac{\mathcal{F}_e(T_e, w_e)}{g(T_e, v)}\right) + \lambda \frac{\partial}{\partial T_e}\left(\frac{v}{g(T_e, v)}\right) = 0 \tag{28}$$

$$\dot{\lambda}(t) = 0 \tag{29}$$

with boundary conditions

$$\begin{aligned} \lambda(t_f) &= -k_s(v_f) \\ v(t_f) &= v_f. \end{aligned} \tag{30}$$

It is clear that the costate $\lambda(t) \equiv -k_s(v_f)$. Combining it with (28), the optimal engine torque $T_e^*(v)$ is a function of the vehicle speed v and final speed v_f, i.e.,

$$T_e^*(v) = h\left(v, k_s(v_f)\right) \tag{31}$$

where h is the function to be determined. Equation (31) shows the fact that the optimal engine torque depends on both vehicle speed v and final speed v_f. Namely, in different departing tasks,

the optimal acceleration and gear position at a specific speed depend on the final speed v_f, which increases the difficulty to determine a proper departing operation.

As a simplification, we set $k_s(v_\mathrm{f})$ to be constant for all departing tasks. Then, λ becomes a constant, and $T_\mathrm{e}^*(v)$ is the function of vehicle speed only as follows:

$$T_\mathrm{e}^*(v) = \tilde{h}(v). \tag{32}$$

This result means that the optimal departing operation is independent of the final speed and is solely determined by the current vehicle speed. With this simplification, a suboptimal algorithm will be derived in the following.

We fixed $k_s(v_\mathrm{f})$ at a constant value $k_s(v_\mathrm{eco})$, where v_eco is the economical cruising speed and then solve the following equation:

$$\frac{\partial H}{\partial T_\mathrm{e}} = \frac{1}{g^2}\left(\frac{\partial \mathcal{F}_\mathrm{e}}{\partial T_\mathrm{e}} g - \mathcal{F}_\mathrm{e}\frac{\partial \}}{\partial T_\mathrm{e}} - \lambda v \frac{\partial g}{\partial T_\mathrm{e}}\right) = 0. \tag{33}$$

When the vehicle accelerate from v to $v + \Delta v$, the equivalent fuel consumption is given by

$$\min_{T_\mathrm{e}} \Delta J = \Delta v \frac{-k_s(v_\mathrm{eco})v + \mathcal{F}_\mathrm{e}(T_\mathrm{e}, w_\mathrm{e})}{a}. \tag{34}$$

The goal of (34) is to find the optimal engine torque to minimize the equivalent fuel consumption E_Δ per unit velocity increment, which is defined as

$$\begin{aligned}\min_{T_\mathrm{e}} E_\Delta &= \lim_{\Delta v \to 0} \frac{\Delta J}{\Delta v} \\ &= \frac{-k_s(v_\mathrm{eco})v + \mathcal{F}_\mathrm{e}(T_\mathrm{e}, w_\mathrm{e})}{g(T_\mathrm{e}, v)}.\end{aligned} \tag{35}$$

By setting $k_s(v_\mathrm{f})$ to $k_s(v_\mathrm{eco})$, the problem in (35) equals to the problem (26) with

$$\frac{\partial E_\Delta}{\partial T_\mathrm{e}} = \frac{\partial H}{\partial T_\mathrm{e}}. \tag{36}$$

In this 1-D optimization problem (35), the optimal engine torque T_e^* can be solved by methods such as steepest descent.

When gear shifting is involved, the optimal gear i_g^* should be selected to minimize E_Δ, i.e.,

$$i_\mathrm{g}^*(v) = \arg\min_{i_\mathrm{g}} \left\{E_\Delta\left(T_\mathrm{e}^*(v, i_\mathrm{g}), i_\mathrm{g}\right)\right\}. \tag{37}$$

The optimal E_Δ and corresponding acceleration of each gear at various speeds are shown in Fig. 8(a). The four intersections of E_Δ are thus the upshifting points.

Fig. 8 shows the mapping between vehicle speed and optimal acceleration/gear position. Namely, it presents a new shift scheduling for accelerating scenarios, which has the potential to improve the calibrated gear-shift scheduling. Automated vehicles can look up this map to determine the acceleration level, gear positions, and gear shifting points. For example, to economically depart from 10 to 20 m/s, gears II, III, and IV are sequentially used, and upshift happens at 12.7 and 18.2 m/s. In application, automated vehicles can directly send the torque/gear-position command to engine/transmission to implement this strategy.

The fuel-consumption increment of this simplified strategy compared with the optimal result is shown in Fig. 8(b). The increment is less than 0.4% when $v_\mathrm{f} \leq 30$ m/s, which covers most departing tasks in real transportation flow. Due to the slightly deteriorated fuel economy and low computing load, this strategy is suitable for online implementation.

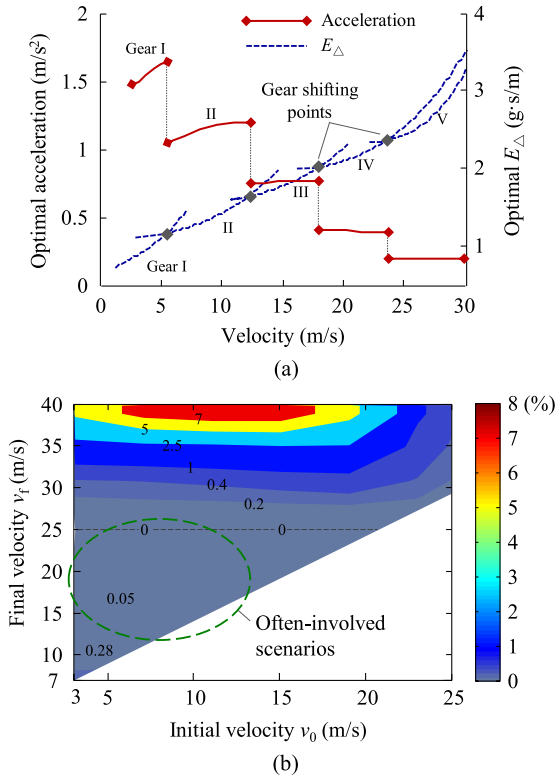

Fig. 8. Near-optimal strategy for online implementation. (a) Optimal E_Δ and optimal acceleration at each gear. (b) Fuel increment (%) of the near-optimal strategy as compared to the optimum.

VI. Eco-Departure for Multiple Vehicles

When multiple vehicles are launching from the same signalized intersection, the first vehicle can apply the economical strategy discussed earlier to depart, while the other vehicles must consider the lead vehicle and their launching might be impeded. Here, we adopt the Gipps car-following model to estimate the maximum safe acceleration $a_{s,n}$ for vehicles behind a lead vehicle [26], i.e.,

$$\begin{aligned}a_{s,n}(t) &= \frac{v_n(t+\tau) - v_n(t)}{\tau} \\ v_n(t+\tau) &= b_n\tau + \Big[b_n^2\tau^2 - 2b_n(x_{n-1} - x_n - D_s) \\ &\qquad + b_n v_n(t)\tau + \frac{b_n v_{n-1}^2}{b_{n-1}}\Big]^{0.5}\end{aligned} \tag{38}$$

where v_n, x_n, and b_n is the speed, location, and expected braking deceleration of vehicle n; τ is the reaction time; D_s is the safe distance of two adjacent vehicles, including the vehicle length. The vehicle information, such as vehicle speed and location, can be exchanged by V2V. Combining $a_{s,n}$ and the economical acceleration $a_{\mathrm{eco},n}$, the applied acceleration is given by

$$a_n(t) = \min(a_{\mathrm{eco},n}, a_{s,n}). \tag{39}$$

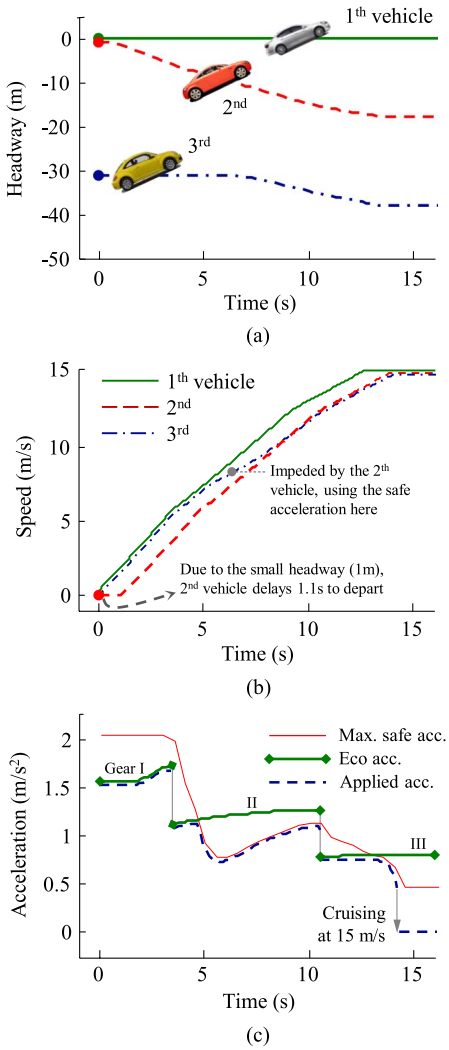

Fig. 9. Eco-departing operation of the platoon with three vehicles. (a) Headway profiles. (b) Vehicle speed profiles. (c) Applied acceleration of the third vehicle.

In the following example, a platoon with three vehicles is considered. The powertrains of the three vehicles are assumed to be the same. The parameters are set as $\tau = 0.55$ s, $D_s = 7.5$ m, and $b_{\#} = -2$ m/s^2. The final speed is 15 m/s. The initial headways are intentionally set to 1 and 30 m to simulate uneven urban driving. The profiles of the headway, acceleration, and speed are shown in Fig. 9.

In Fig. 9(a), the headway of the second vehicle becomes larger as the vehicle speed increases. Since the initial gap is small, the start-up of the second vehicle delays 1.07 s first, and then, it follows the economical acceleration profile to depart, as shown in Fig. 9(b). The third vehicle has a large initial headway and can accelerate without being unimpeded initially, as shown in Fig. 9(c). When it closes to the second vehicle, it utilizes a lower safe acceleration to avoid collision risk. The applied acceleration actually deviates from the economical acceleration and thus may lead to a worse fuel economy. The equivalent fuel consumptions of the three vehicles are 14.94, 14.98, and 15.28 g, meaning that the second vehicle with a short delay achieved a similar fuel economy with the first vehicle, while the third vehicle consumed 2.3% more fuel due to the impediment of its front vehicle, even if it has a large initial headway.

The aforementioned results also indicate the limitation of this strategy, i.e., the lack of prediction and synthesized optimization, which means that it cannot ensure the optimality of all vehicles. However, this strategy is practical and reasonable for automated vehicles because it does not need online time-costly optimization and prediction of leading vehicles' trajectory, particularly in the early intelligent transportation systems where automated and unpredictable human-driven vehicles are coexistent.

VII. Conclusion

This paper studied the fuel-optimal departing operation of connected vehicles at signalized intersections. A Bolza-type OCP with the goal of maximizing fuel economy was formulated. The Legendre pseudospectral method and knotting technique was used to solve the optimization problem.

It is found that 1) the fuel-optimal acceleration does not simply operate the engine on its BSFC line and, instead, must be optimized to maximize the overall system efficiency; 2) at the beginning of eco-departure, the "kick-down" strategy could result in better fuel performance; 3) a near-optimal eco-departure strategy can be (and was) developed to very fast determine the acceleration profile, gear positions, and gear shifting points with increasing fuel consumption slightly; 4) the eco-departure issue of being impeded by lead vehicles can be addressed by combining a safety-bounded car-following model and the proposed eco-departing strategy.

Generally, eco-driving has the potential to save fuel for connected vehicles, but its realization requires accurate control of the engine and transmission, which can be executed more accurately by automatic control systems and less so by human drivers. It is worth noting that other factors, such as road slope, also impact the implementation of eco-driving, which were not considered in this paper.

References

[1] E. Uhlemann, "Introducing connected vehicles," *IEEE Veh. Technol. Mag.*, vol. 10, no. 1, pp. 23–31, Mar. 2015.
[2] N. Lu, N. Cheng, N. Zhang, X. Shen, and J. W. Mark, "Connected vehicles: Solutions and challenges," *IEEE Internet Things J.*, vol. 1, no. 4, pp. 289–299, Aug. 2014.
[3] A. B. Reis, S. Sargento, F. Neves, and O. K. Tonguz, "Deploying roadside units in sparse vehicular networks: What really works and what does not," *IEEE Trans. Veh. Technol.*, vol. 63, no. 6, pp. 2794–2806, Jul. 2014.
[4] J. N. Barkenbus, "Eco-driving: An overlooked climate change initiative," *Energy Policy*, vol. 38, no. 2, pp. 762–769, Feb. 2010.
[5] A. E. Atabani, I. A. Badruddin, S. Mekhilef, and A. S. Silitonga, "A review on global fuel economy standards, labels and technologies in the transportation sector," *Renew. Sustainable Energy Rev.*, vol. 15, no. 9, pp. 4586–4610, Dec. 2011.
[6] K. Boriboonsomsin, M. Barth, and A. Vu, "Evaluation of driving behavior and attitude towards eco-driving: A Southern California limited case study," in *Proc. 90th Annu. Meet. Transp. Res. Board*, Washington, DC, USA, 2011, pp. 1–14.
[7] M. Barth and K. Boriboonsomsin, "Energy and emissions impacts of a freeway-based dynamic eco-driving system," *Transp. Res. D, Transp. Environ.*, vol. 14, no. 6, pp. 400–410, Aug. 2009.
[8] G. De Nunzio, C. Canudas de Wit, P. Moulin, and D. Di Domenico, "Eco-driving in urban traffic networks using traffic signal information," in *Proc. IEEE 52nd Annu. CDC*, 2013, pp. 892–898.

[9] E. Hellström, M. Ivarsson, J. Åslund, and L. Nielsen, "Look-ahead control for heavy trucks to minimize trip time and fuel consumption," *Control Eng. Pract.*, vol. 17, no. 2, pp. 245–254, Feb. 2009.
[10] M. A. S. Kamal, M. Mukai, J. Murata, and T. Kawabe, "Ecological vehicle control on roads with up-down slopes," *IEEE Trans. Intell. Transp. Syst.*, vol. 12, no. 3, pp. 783–794, Sep. 2011.
[11] S. Xu, S. E. Li, K. Deng, S. Li, and B. Cheng, "A unified pseudospectral computational framework for optimal control of road vehicles," *IEEE/ASME Trans. Mechatronics*, vol. 20, no. 4, pp. 1499–1510, Aug. 2015.
[12] M. Alsabaan, K. Naik, and T. Khalifa, "Optimization of fuel cost and emissions using V2V communications," *IEEE Trans. Intell. Transp. Syst.*, vol. 14, no. 3, pp. 1449–1461, Sep. 2013.
[13] T. Tielert *et al.*, "The impact of traffic-light-to-vehicle communication on fuel consumption and emissions," in *Proc. IEEE IOT*, 2010, pp. 1–8.
[14] G. Thomas and P. G. Voulgaris, "Fuel minimization of a moving vehicle in suburban traffic," in *Proc. ACC*, 2013, pp. 4009–4014.
[15] B. Asadi and A. Vahidi, "Predictive cruise control: Utilizing upcoming traffic signal information for improving fuel economy and reducing trip time," *IEEE Trans. Control Syst. Technol.*, vol. 19, no. 3, pp. 707–714, May 2011.
[16] D. Yamaguchi, M. A. S. Kamal, M. Mukai, and T. Kawabe, "Model predictive control for automobile ecological driving using traffic signal information," *J. Syst. Des. Dyn.*, vol. 6, no. 3, pp. 297–309, 2012.
[17] S. Mandava, K. Boriboonsomsin, and M. Barth, "Arterial velocity planning based on traffic signal information under light traffic conditions," in *Proc. IEEE Conf. Intell. Transp. Sys.*, 2009, pp. 1–6.
[18] H. Rakha and R. K. Kamalanathsharma, "Eco-driving at signalized intersections using V2I communication," in *Proc. 14th IEEE ITSC*, 2011, pp. 341–346.
[19] M. Soler, A. Olivares, and E. Staffetti, "Hybrid optimal control approach to commercial aircraft trajectory planning," *J. Guid. Control Dyn.*, vol. 33, no. 3, pp. 985–991, May/Jun. 2010.
[20] S. Li, S. Xu, W. Wang, and B. Cheng, "Pseudospectral optimization of economical accelerating strategy for vehicles with discontinuous gear ratio," *Acta Autom. Sinica*, vol. 41, no. 3, pp. 475–485, 2015.
[21] M. Hu, "Study on energy management strategy for mild hybrid electrical vehicle with CVT," Ph.D. dissertation, Dept. Mech. Eng., Chongqing Univ., Chongqing, China, 2007.
[22] G. Elnagar, M. A. Kazemi, and M. Razzaghi, "The Legendre pseudospectral method for discretizing optimal control problems," *IEEE Trans. Autom. Control*, vol. 40, no. 10, pp. 1793–1796, Oct. 1995.
[23] I. M. Ross and F. Fahroo, "Pseudospectral knotting methods for solving non-smooth optimal control problems," *J. Guid. Control Dyn.*, vol. 27, no. 3, pp. 397–405, May/Jun. 2004.
[24] F. Fahroo and I. M. Ross, "Advances in pseudospectral methods for optimal control," in *Proc. AIAA Guid., Navig. Control Conf. Exhib.*, Honolulu, HI, USA, 2008, pp. 18–21.
[25] P. E. Gill, W. Murray, and M. A. Saunders, "SNOPT: An SQP algorithm for large-scale constrained optimization," *SIAM Rev.*, vol. 47, no. 1, pp. 99–131, 2005.
[26] P. G. Gipps, "A behavioural car-following model for computer simulation," *Transp. Res. B, Methodol.*, vol. 15, no. 2, pp. 105–111, Apr. 1981.

Shengbo Eben Li (M'11) received the M.S. and Ph.D. degrees in automotive engineering from Tsinghua University, Beijing, China, in 2006 and 2009, respectively.

In 2007, he was a Visiting Researcher with Stanford University, Stanford, CA, USA, and from 2009 to 2011, he was a Postdoctoral Research Fellow with the University of Michigan, Ann Arbor, MI, USA. He is currently an Associate Professor with the Department of Automotive Engineering, Tsinghua University. His active research interests include autonomous vehicle control, optimal and predictive control, driver-assistance systems, lithium ion battery management, etc.

Dr. Li received the Award for Science and Technology from the China Intelligent Transportation Systems Association (2012), the Award for Technological Invention from the Ministry of Education (2012), the National Award for Technological Invention in China (2013), and the Honored Funding for Beijing Excellent Youth Researcher Award (2013).

Shaobing Xu received the B.S. degree in automotive engineering from the China Agricultural University, Beijing, China, in 2011. He is currently working toward the Ph.D. degree in automotive engineering with Tsinghua University, Beijing.

His research interest includes optimal control theory and vehicle dynamics control.

Mr. Xu has received several awards and honors, including the National Scholarship, the President Scholarship, the First Prize from the Chinese Fourth Mechanical Design Contest, and the First Prize from the 19th Advanced Mathematical Contest.

Xiaoyu Huang received the B.E. degree in automotive engineering from Tsinghua University, Beijing, China, in 2009 and the Ph.D. degree in mechanical and aerospace engineering from The Ohio State University, Columbus, OH, USA, in 2014.

He is currently a Researcher with General Motors Research and Development, Warren, MI, USA. He is the author or coauthor of over 20 peer-reviewed journal and conference papers. His research interests include vehicle dynamics, control, estimation, diagnosis, and prognosis, specifically for chassis control systems, active safety features, and electric vehicles.

Bo Cheng received the B.S. and M.S. degrees in automotive engineering from Tsinghua University, Beijing, China, in 1985 and 1988, respectively, and the Ph.D. degree in mechanical engineering from Tokyo University, Tokyo, Japan, in 1998.

He is currently a Professor with Tsinghua University, where he is also the Dean of the Tsinghua University Suzhou Automotive Research Institute. His active research interests include autonomous vehicles, driver-assistance systems, active safety, vehicular ergonomics, etc.

Dr. Cheng serves as the Chairman of the Academic Board of the Society of Automotive Engineers in Beijing, a Council Member of the Chinese Ergonomics Society, a Committee Member of the National 863 Plan, among others.

Huei Peng received the Ph.D. degree in mechanical engineering from the University of California at Berkeley, Berkeley, CA, USA, in 1992.

He is currently a Professor with the Department of Mechanical Engineering, University of Michigan, Ann Arbor, MI, USA. He is also a Changjiang Scholar with Tsinghua University, Beijing, China. His research interests include adaptive control and optimal control, with emphasis on their applications to vehicular and transportation systems. His current research focus includes the design and control of electrified vehicles and connected/automated vehicles.

Dr. Peng is a Fellow of both the Society of Automotive Engineers and the American Society of Mechanical Engineers.